AGU PUBLICATIONS

Geophysical Research Letters

RESEARCH LETTER
10.1002/2017GL073465

Key Points:
- Water-saturated Na-montmorillonite gouge has a very low frictional strength at temperatures up to 150°C
- Temperature has a stabilizing effect on frictional sliding of Na-montmorillonite under hydrothermal conditions
- Fluid-rich, montmorillonite-rich décollements are unlikely to be nucleation sites for earthquake rupture

Supporting Information:
- Supporting Information S1

Correspondence to:
K.-i. Hirauchi,
hirauchi.kenichi@shizuoka.ac.jp

Citation:
Mizutani, T., K.-i. Hirauchi, W. Lin, and M. Sawai (2017), Depth dependence of the frictional behavior of montmorillonite fault gouge: Implications for seismicity along a décollement zone, *Geophys. Res. Lett.*, *44*, 5383–5390, doi:10.1002/2017GL073465.

Received 14 MAR 2017
Accepted 18 MAY 2017
Accepted article online 22 MAY 2017
Published online 3 JUN 2017

Depth dependence of the frictional behavior of montmorillonite fault gouge: Implications for seismicity along a décollement zone

Tomoyo Mizutani[1], Ken-ichi Hirauchi[2], Weiren Lin[3,4], and Michiyo Sawai[5]

[1]Department of Science, Graduate School of Integrated Science and Technology, Shizuoka University, Shizuoka, Japan, [2]Department of Geosciences, Faculty of Science, Shizuoka University, Shizuoka, Japan, [3]Graduate School of Engineering, Kyoto University, Kyoto, Japan, [4]Kochi Institute for Core Sample research, Japan Agency for Marine-Earth Science and Technology, Nankoku, Japan, [5]Department of Earth Sciences, Chiba University, Chiba, Japan

Abstract To understand the seismogenic potential of shallow plate-boundary thrust faults (décollements) in relatively warm subduction zones, water-saturated Na-montmorillonite gouges were sheared at a pore fluid pressure of 10 MPa, effective normal stresses (σ_n^{eff}) of 10–70 MPa, temperatures (T) of 25–150°C, and axial displacement rates of 0.03–3 μm/s. The Na-montmorillonite gouges were frictionally very weak at all conditions tested (steady state friction coefficient μ_{ss} = 0.05–0.09). At $T \leq 60$°C, Na-montmorillonite showed a transition from velocity-strengthening to velocity-weakening behavior with increasing σ_n^{eff}, whereas at $T \geq 90$°C it was largely velocity neutral or velocity strengthening, irrespective of σ_n^{eff}. The rates of frictional healing (β) showed extremely low values (mostly <0.001) at all temperatures. Our results suggest that the existence of Na-montmorillonite in the décollement zone at Costa Rica and Nankai promotes aseismic slip, particularly at shallow depths, forming weakly coupled regions.

1. Introduction

Most of the large and great earthquakes on Earth occur along the plate boundaries of subduction zones [e.g., *Dixon and Moore*, 2007]. In a relatively warm subduction zone (e.g., Costa Rica and Nankai), the shallow plate boundary thrust (i.e., décollement) is considered aseismic at depths shallower than 10 km [e.g., *Park et al.*, 2002; *Ranero et al.*, 2008; *Tobin and Saffer*, 2009], thereby inhibiting earthquake rupture nucleation. However, recent geophysical observations have revealed the occurrence of slow earthquakes within shallow accretionary prisms (including the décollements) [e.g., *Ito and Obara*, 2006; *Wallace and Beavan*, 2010; *Davis et al.*, 2015]. Therefore, understanding the frictional properties of the décollement is important for assessing seismic hazards.

The décollement zone forms within clay-rich (up to 90 wt %) pelagic and hemipelagic sediments on a subducting oceanic plate [e.g., *Deng and Underwood*, 2001; *Underwood*, 2007; *Saffer et al.*, 2008; *Kameda et al.*, 2015]. Smectites, a group of 2:1 layer swelling clay minerals, are known as major constituents of the clay-rich horizon. Smectites retain variable amounts of water within the interlayer space, in which the number of water molecules bound to cations increases with increasing relative humidity (one- to three-layer hydrates) [*Sposito and Prost*, 1982]. In addition, when saturated with water, the structure of interlayer molecules tumbles and approaches that in aqueous solution. Therefore, water content is an important factor in controlling their frictional properties [e.g., *Ikari et al.*, 2007]. Previous friction experiments have shown that hydrated (three-layer hydrate) and water-saturated montmorillonite gouges have anomalously low strengths [e.g., *Logan and Rauenzahn*, 1987; *Ikari et al.*, 2007; *Moore and Lockner*, 2007; *Behnsen and Faulkner*, 2012, 2013], with coefficients of friction as low as 0.03. The velocity dependence of friction ($a-b$) for montmorillonites varies with water content at a given normal stress, whereby hydrated samples exhibit velocity-weakening or velocity-strengthening behavior [*Saffer and Marone*, 2003; *Ikari et al.*, 2007], while water-saturated samples generally show velocity strengthening [e.g., *Tembe et al.*, 2010].

Smectite is mineralogically stable at temperatures up to 150°C [*Pytte and Reynolds*, 1988], above which it transforms to illite clay. This transition may be responsible for the onset of seismicity along the subduction thrust [*Vrolijk*, 1990; *Hyndman et al.*, 1997]. *den Hartog et al.* [2012] and *den Hartog and Spiers* [2013] have shown that ($a-b$) for illite gouge depends strongly on effective normal stress and temperature. As smectite and illite are both 2:1 layer aluminosilicates [*Colten-Bradley*, 1987], smectite is also likely to show pressure-

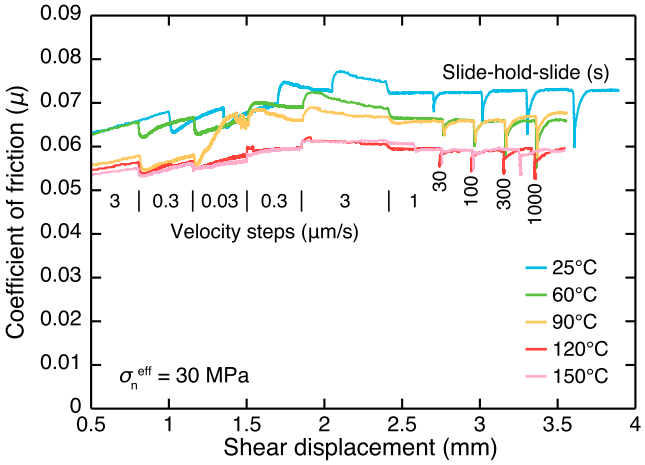

Figure 1. Coefficient of friction (μ) as a function of shear displacement for Na-montmorillonite samples sheared at a pore fluid pressure of 10 MPa, an effective normal stress of 30 MPa, and temperatures (T) of 25–150°C. Note that at T = 90°C, pronounced increases in μ occur during the 0.03 μm/s velocity step, in which case ($a-b$) was not calculated.

and temperature-dependent frictional behavior. Although *Saffer and Marone* [2003] and *Ikari et al.* [2007] have indeed shown that for hydrated montmorillonite gouges, increasing normal stress causes a transition from velocity weakening to velocity strengthening, previous friction experiments on montmorillonite clay, including those mentioned above, have all been conducted at room temperature. In this study, therefore, we conducted low- to high-temperature (25–150°C) friction experiments at subseismic slip rates on water-saturated montmorillonite gouge over a range of effective normal stresses (10–70 MPa), with the aim of understanding how fault strength and frictional stability change with increasing depth. We discuss the influence of montmorillonite friction on the inhibition of great earthquakes along the décollement of a subduction zone.

2. Experimental methods

All experiments were performed in a triaxial deformation apparatus installed at the Kochi Institute for Core Sample Research, Japan (Text S1 and Figure S1 in the supporting information). A silicone oil was used as the confining medium and deionized water as the pore fluid. A schematic diagram of the sample assembly is shown in Figure S2. Simulated fault gouges used in this study were prepared from powders of bentonite (Na-montmorillonite), purchased from the Clay Science Society of Japan (JCSS3101) [*Miyawaki et al.*, 2010]. An initially ~3 mm thick layer of Na-montmorillonite gouge (<106 μm in particle size) was placed between two forcing blocks of Indian sandstone (11%–14% porosity and 10^{-16} to 10^{-15} m^2 permeability) [*Tanikawa et al.*, 2012] with diameters of 40 mm and lengths of 95 mm, precut at angles of 30° from the maximum compression direction. The precut surfaces were roughened with #100 SiC abrasive to ensure good coupling between the forcing blocks and the gouge layer. For pore fluid entry, a borehole of ~3 mm in diameter was drilled perpendicular to the precut surfaces in the forcing blocks. Before being lowered into the pressure vessel, the piston-sample assembly was placed inside a heat-shrinkable fluororesin jacket to isolate it from the confining medium.

Friction experiments were conducted at a pore fluid pressure of 10 MPa, effective normal stresses (σ_n^{eff}) of 10, 30, 50, and 70 MPa and temperatures (T) of 25, 60, 90, 120, and 150°C, under drained conditions. The samples were kept at a normal stress of 20 MPa and a pore fluid pressure of 10 MPa for at least 3 h before the initiation of shearing, allowing equilibration of the sample with the pore fluid. The gouge layer was initially sheared at an axial displacement rate of 3 μm/s until an approximate shear displacement of 0.8 mm was reached, after which the axial displacement rate was systematically changed to 0.3, 0.03, 0.3, 3, and finally 1 μm/s (Figure S3). Following these velocity step tests, we performed slide-hold-slide (SHS) tests, during which the layer was sheared at 1 μm/s, held motionless for a prescribed time t_h (30, 100, 300, and 1000 s), then subjected to shear again. Details of the experimental conditions and key mechanical data are provided in Table S1.

Since the smectite clays are frictionally very weak [e.g., *Moore and Lockner*, 2007], we have performed a series of calibration tests to determine the strength of the fluororesin jacket at each σ_n^{eff}-T condition. The contributions from the jacket strength (and changes in contact area between the forcing blocks during deformation) were subtracted from the law data to obtain true shear stress values of Na-montmorillonite (see Text S2 for details). We define the coefficient of friction (μ) as the ratio of shear stress to effective normal stress, assuming zero cohesion. The velocity dependence of friction is quantified using the friction rate parameter, $(a-b) = \Delta\mu_{ss}/\Delta \ln V$, where μ_{ss} is the steady state friction coefficient and V is the sliding velocity [e.g.,

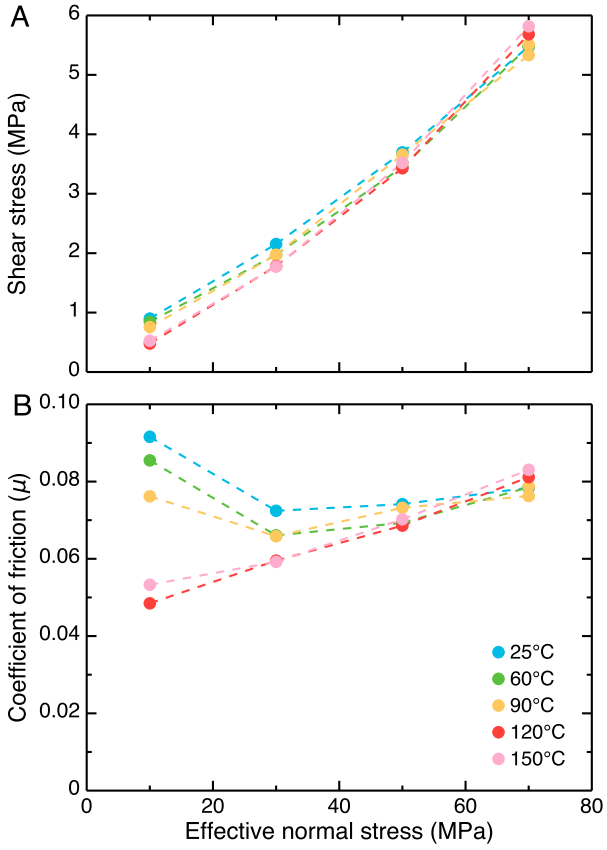

Figure 2. Summary of friction data for Na-montmorillonite sheared at temperatures of 25–150°C. All plotted measurements were taken at 2.60–2.78 mm shear displacement. (a) Shear stress versus effective normal stress. (b) Coefficient of friction (μ) versus effective normal stress.

Marone, 1998a]. Positive ($a-b$) values indicate an increase in μ with increasing velocity (i.e., velocity-strengthening slip behavior), which is inherently stable. Negative ($a-b$) values mean that the behavior is velocity weakening, which is potentially unstable. The effect of strain hardening was corrected by applying a linear detrending for each velocity step, following *Blanpied et al.* [1998]. The rate of frictional healing (β) is given by $\Delta\mu/\log t_h$, where $\Delta\mu$ is the difference between peak friction following a hold and the peak steady state friction prior to the hold.

3. Results

Figure 1 shows the coefficient of friction (μ) as a function of shear displacement for Na-montmorillonite gouge deformed at an effective normal stress of 30 MPa and temperatures of 25–150°C. All samples show strain hardening toward steady state shear stress at ~2 mm displacement. The steady state shear stress value obtained at 2.60–2.78 mm displacement (just before the initiation of SHS tests) increases almost linearly with effective normal stress at each temperature (Figure 2a). Plots of the steady state coefficient of friction (μ_{ss}) versus effective normal stress are shown in Figure 2b, for temperatures between 25 and 150°C. For all samples, μ_{ss} ranges from 0.048 to 0.091. μ_{ss} gradually increases with increasing effective normal stress, except that at temperatures

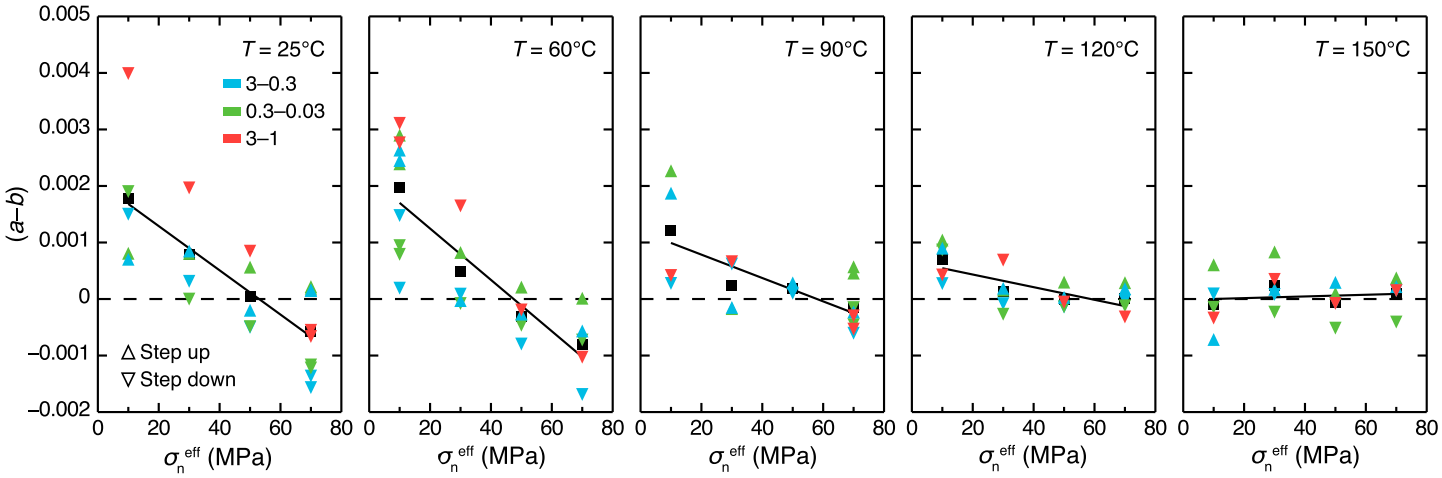

Figure 3. Plots of the friction rate parameter ($a-b$) as a function of effective normal stress (σ_n^{eff}) for Na-montmorillonite sheared at temperatures of 25–150°C. Different velocity steps (μm/s) were plotted by the triangles with different colors (see the legend in the left-hand panel). The black squares represent an average value of all velocity steps at each σ_n^{eff}.

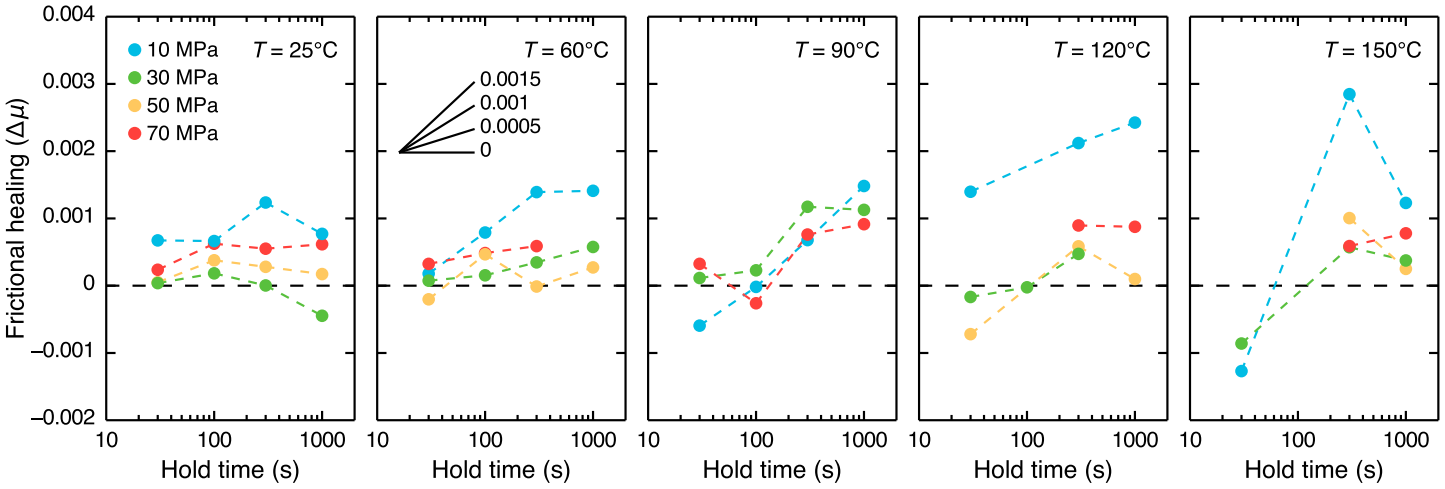

Figure 4. Plots of frictional healing ($\Delta\mu$) as a function of hold time for Na-montmorillonite sheared at temperatures of 25–150°C. Different effective normal stresses are plotted with different colors (see the legend in the left-hand panel).

of ≤90°C, the μ_{ss} values at σ_n^{eff} = 10 MPa are higher than those at 30 MPa. This trend can be explained by the existence of cohesion in the samples sheared at lower temperatures (Figure 2a). Variations in μ_{ss} at a given σ_n^{eff} become larger at lower effective normal stress (Figure 2b).

Values of ($a-b$) for Na-montmorillonite gouge are plotted as a function of effective normal stress in Figure 3: all samples show values ranging from –0.0017 to 0.0040, essentially independent of sliding velocity (Figures 3 and S4). At temperatures of 25 and 60°C, the average ($a-b$) values at a given σ_n^{eff} steadily decrease with increasing effective normal stress. At temperatures of ≥90°C, however, they show only a weak negative dependence on effective normal stress; in particular, the average ($a-b$) values are roughly constant at

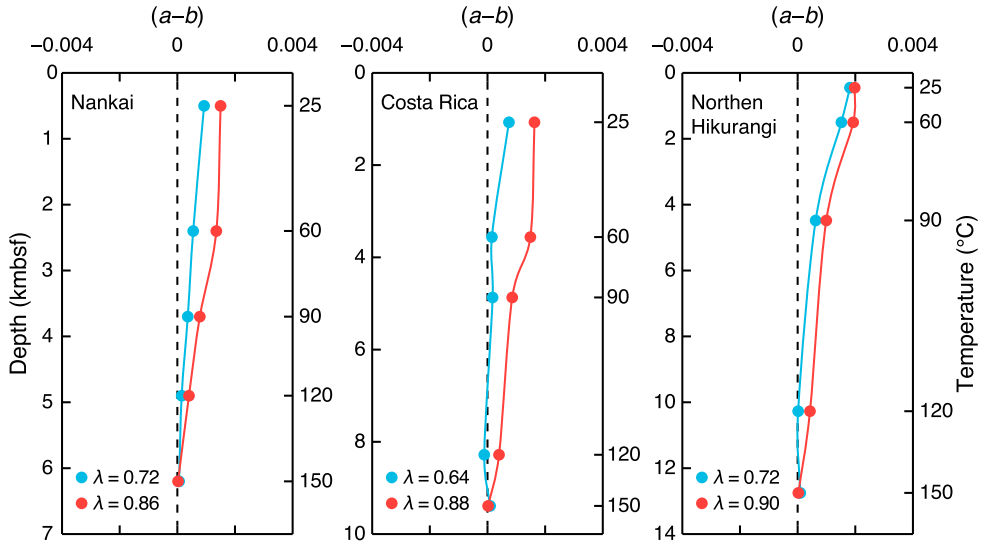

Figure 5. Calculated friction rate parameters ($a-b$) as functions of depth for décollements at Costa Rica, Nankai, and northern Hikurangi, at pore fluid pressure ratios (λ) of 0.64–0.88 [*Spinelli et al.*, 2006], 0.72–0.87 [*Kitajima and Saffer*, 2012], and 0.72–0.90 [*Bassett et al.*, 2014; *Ellis et al.*, 2015], respectively. For simplicity, the coefficient of friction for the décollements is fixed at 0.071, which is an average value at σ_n^{eff} = 50 MPa (Table S1). Although the choice of μ in the range of 0.05–0.09 (Table S1) is arbitrary, it does not significantly influence σ_n^{eff} at depth. Values of ($a-b$) at depth were obtained by assuming a linear relationship between ($a-b$) and effective normal stress at each temperature tested (i.e., 25, 60, 90, 120, and 150°C; Figure 3). The normal stress and plate interface depth at each temperature were estimated based on the wedge geometry and thermal structure determined by *Ranero et al.* [2008] for Costa Rica, *Park et al.* [2002] and *Saffer and Tobin* [2011] for Nankai, and *Ellis et al.* [2015] for northern Hikurangi. The density of the accretionary wedge is taken to be 2.0 kg/m^3 [*Gettemy and Tobin*, 2003; *Expedition 316 Scientists*, 2009].

effective normal stresses of ≥30 MPa and a temperature of 150°C. The SHS tests show that values of frictional healing ($\Delta\mu$) range from –0.0013 to 0.0028, indicating a weak positive dependence on hold time at higher temperatures (Figure 4). The rates of frictional healing (β) are in the range –0.0003 to 0.0020, which is at least 1 order of magnitude lower than the healing rates of quartz gouges [*Marone*, 1998b].

4. Discussion and Conclusions

Our friction experiments indicate that fault strength and frictional stability for wet Na-montmorillonite depend on effective normal stress and temperature. We first compare friction values from our experiments with those of montmorillonite gouges deformed at room temperature. The observed linear increase in shear stress with effective normal stress (Figure 2a) indicates that shear deformation was purely frictional under our experimental conditions. This observation is in contrast with previous experiments on hydrated Ca-montmorillonite gouge (three-layer hydrate), in which the Mohr-Coulomb failure envelope exhibited "rollover" at σ_n^{eff} = 25–40 MPa [*Ikari et al.*, 2007]. As discussed by *Moore and Lockner* [2007], the transition to pressure-insensitive deformation in montmorillonite may be caused by the development of fluid overpressures within the low-permeability clay gouge, because of the use of impermeable steel forcing blocks. The steady state friction coefficient of our samples ranged from 0.07 to 0.09, which lies almost entirely within the range of water-saturated Na-montmorillonite gouges under conditions of similar effective normal stress (μ = 0.08–0.16 at σ_n^{eff} = 5–100 MPa) [*Logan and Rauenzahn*, 1987; *Morrow et al.*, 1992; *Brown et al.*, 2003; *Moore and Lockner*, 2007; *Takahashi et al.*, 2007; *Tembe et al.*, 2010; *Behnsen and Faulkner*, 2012, 2013].

Our friction values at all temperatures show that at $\sigma_n^{eff} \geq 30$ MPa, the coefficient of friction increases with increasing effective normal stress (Figures 2b). This trend can be explained by a decrease in the thicknesses of water films absorbed into the montmorillonite (001) surfaces [*Moore and Lockner*, 2007; *Behnsen and Faulkner*, 2012, 2013]. Similar trends have been observed for other phyllosilicates, such as chrysolite, illite, and muscovite [*Moore et al.*, 2004; *Behnsen and Faulkner*, 2012].

At room temperature, our water-saturated Na-montmorillonite gouges exhibit a transition from velocity-strengthening to velocity-weakening behavior at σ_n^{eff} = 50 MPa (Figure 3). The decrease in ($a-b$) with increasing effective normal stress has been reported for quartz gouge sheared at normal stresses in the range of 50–190 MPa [*Marone and Scholz*, 1988; *Marone et al.*, 1990]. Increasing effective normal stress leads to an increase in consolidation state of gouge, which may act to decrease ($a-b$) values [*Scholz*, 1998]. In contrast, for hydrated Ca-montmorillonite gouges (one- to three-layer hydrates) sheared at sliding velocities of 1–20 μm/s, values of ($a-b$) changes from negative to positive at σ_n = 30–40 MPa [*Saffer and Marone*, 2003; *Ikari et al.*, 2007]. Although the reason for the contrast in trends of (a–b) with σ_n^{eff} is unclear, we suggest that the positive ($a-b$) values at $\sigma_n > 40$ MPa are attributed to the development of fluid overpressures [*Moore and Lockner*, 2007], where the consolidation state of the gouge remains low at high applied normal stresses. Previous friction experiments have shown that water-saturated Na-montmorillonite gouges are dominantly velocity strengthening at σ_n^{eff} = 5–40 MPa [*Brown et al.*, 2003; *Tembe et al.*, 2010], which is consistent with our results.

Our results show that with increasing temperature, the observed dependence of ($a-b$) on effective normal stress for water-saturated montmorillonite gouge changes from negative to flat (Figures 3 and S4). Furthermore, at higher temperatures (≥120°C), mostly velocity-neutral or velocity-strengthening behaviors are observed for water-saturated montmorillonite gouges, except for some of the downward velocity step data. This suggests that temperature has a stabilizing effect on the frictional sliding of Na-montmorillonite under hydrothermal conditions, although the magnitude of ($a-b$) is very small (mostly <0.001 at $T \geq$120°C).

The rates of frictional healing for wet Na-montmorillonite were extremely low (mostly $\beta < 0.001$; Figure 4), implying essentially no growth of real contact areas during holds [*Tesei et al.*, 2012]. Similar healing rates have been reported for wet clays of chlorite and saponite [*Katayama et al.*, 2015], and natural clay-rich or phyllosilicate-rich samples collected from the San Andreas Fault [*Carpenter et al.*, 2011] and the Zuccale Fault [*Tesei et al.*, 2014]. This lack of frictional healing is attributed to the alignment of (001) planes in phyllosilicates, which induces saturation of the real contact area during shearing [*Tesei et al.*, 2012]. We therefore suggest that the existence of Na-montmorillonites within fault zones leads to a slow strength recovery after fault slip, and thus to low values of shear stress throughout the seismic cycle. However, this must be treated with some caution because recent SHS tests show that quartz- and phyllosilicate-rich gouges exhibit significantly higher healing rates at hold times of >3000 s [*Ikari et al.*, 2016]. Given that the maximum hold time in

the present study was only 1000 s, further experiments at longer hold times are required to investigate whether montmorillonite shows power law healing under hydrothermal conditions.

In subduction zones, effective normal stress and temperature at depth are strongly dependent on pore fluid pressure and the taper angle of the accretionary prism [*Saffer and Bekins*, 2006; *Wang and Hu*, 2006]. Assuming (1) a décollement composed of 100% Na-montmorillonite and (2) a linear relationship between $(a-b)$ and effective normal stress at each temperature (Figure 3), we calculated a depth profile for $(a-b)$ along a plate boundary thrust in three subduction zones (Costa Rica, Nankai, and northern Hikurangi) (Figure 5). For the décollements at Costa Rica, Nankai and northern Hikurangi, the pore fluid pressure ratio λ was estimated to be 0.64–0.88, 0.72–0.87, and 0.72–0.90, respectively [*Moore and Saffer*, 2001; *Spinelli et al*., 2006; *Kitajima and Saffer*, 2012; *Bassett et al*., 2014; *Ellis et al*., 2015; *Saffer and Wallace*, 2015]; however, it is important to note that the effect of pore fluid pressure on $(a-b)$ [e.g., *Scuderi and Collettini*, 2016] is neglected in the depth profile. Our calculations show that for the three subduction zone settings, a Na-montmorillonite fault zone exhibits velocity-strengthening or velocity-neutral behavior at all depths where smectite is mineralogically stable (i.e., $T < 150$°C). At depths where temperatures are ≤120°C, higher λ leads to higher $(a-b)$. We also found that the consolidation state of the décollements remains too low to promote slip instability, although $(a-b)$ tends to decrease toward neutral values with increasing depth.

We note that slip behaviors of the décollements may vary depending on the amount of terrigenous sediments (i.e., quartz and feldspar), particularly at elevated temperatures ($T \geq 120$°C) where montmorillonite (smectite clay) exhibits nearly velocity-neutral behavior (Figure 3). At Nankai, for example, the total clay content in the décollement zone ranges from 50 to 70 wt % [*Underwood*, 2007; *Saffer et al*., 2008]. Therefore, in order to construct a more realistic $(a-b)$ versus depth profile, it is important to investigate how frictional properties of the décollement material change as a function of clay content, under hydrothermal, in situ σ_n^{eff}-T conditions.

Overpressurized fluids that lead to higher λ must play a major role in controlling the occurrence of shallow slow earthquakes in subduction zones [e.g., *Kitajima and Saffer*, 2012; *Bassett et al*., 2014]. Although in northern Hikurangi, slow slip events (SSEs) occur close to the trench (at depths of <2 km [*Wallace et al*., 2016]; the linear relation between $(a-b)$ and σ_n^{eff} at $T \leq 90$°C (Figure 3) implies that Na-montomorillonite in the décollements exhibits velocity-strengthening behavior at the low temperatures and pressures. We therefore suggest that SSEs near the trench are generated by geological heterogeneities within a fault zone characterized by mixed rate- and state-dependent frictional properties [*Skarbek et al*., 2012; *Fagereng et al*., 2014], although we do not preclude the possibility that an increase in pore fluid pressure at a given normal stress results in slip instability, as seen in shear experiments on carbonate gouges [*Scuderi and Collettini*, 2016]. On the other hand, most shallow earthquakes in Nankai and northern Hikurangi have been observed at deeper depths [*Saffer and Wallace*, 2015]. Our results indicate that at $T \geq 120$°C, the frictional behavior of Na-montmorillonite in the décollement zone becomes velocity neutral irrespective of effective normal stress, providing a favorable condition for slow slip [e.g., *Liu and Rice*, 2005].

Acknowledgments
We appreciate Kentaro Hatakeda's technical support while conducting the experiments. Miki Takahashi kindly provided grease and Teflon sheets used for calibration tests. We thank Ikuo Katayama and Yohei Hamada for helpful comments and discussions. We greatly appreciate constructive comments by Diane Moore and two anonymous reviewers, as well as careful editorial handling by Andrew Newman and Åke Fagereng. This study was funded by a Grant-in-Aid for Scientific Research on Innovative Areas (26109005) and the Ministry of Education, Culture, Sports, Science and Technology (MEXT) of Japan, under its Earthquake and Volcano Hazards Observation and Research Program. Supporting data are included as one table in a supporting information file; any additional data may be obtained from K.H. (email: hirauchi.kenichi@shizuoka.ac.jp).

References

Bassett, D., R. Sutherland, and S. Henrys (2014), Slow wave speeds and fluid overpressure in a region of shallow geodetic locking and slow slip, Hikurangi subduction margin, New Zealand, *Earth Planet. Sci. Lett.*, *389*, 1–13, doi:10.1016/j.epsl2013.12.021.

Behnsen, J., and D. R. Faulkner (2012), The effect of mineralogy and effective normal stress on frictional strength of sheet silicates, *J. Struct. Geol.*, *42*, 49–61, doi:10.1016/j.jsg.2012.06.015.

Behnsen, J., and D. R. Faulkner (2013), Permeability and frictional strength of cation-exchanged montmorillonite, *J. Geophys. Res. Solid Earth.*, *118*, 1–11, doi:10.1002/jgrb.50226.

Blanpied, M. L., C. J. Marone, D. A. Lockner, J. D. Byerlee, and D. P. King (1998), Quantitative measure of the variation in fault rheology due to fluid-rock interactions, *J. Geophys. Res.*, *103*, 9691–9712, doi:10.1029/98JB00162.

Brown, K. M., A. Kopf, M. B. Underwood, and J. L. Weinberger (2003), Compositional and fluid pressure controls on the state of stress on the Nankai subduction thrust: A weak plate boundary, *Earth Planet. Sci. Lett.*, *214*, 589–603, doi:10.1016/S0012-821X(03)00388-1.

Carpenter, B. M., C. Marone, and D. M. Saffer (2011), Weakness of the San Andreas Fault revealed by samples from the active fault zone, *Nat. Geosci.*, *4*, 251–254, doi:10.1038/ngeo1089.

Colten-Bradley, V. A. (1987), Role of pressure in smectite dehydration—Effects on geopressure and smectite-to-illite transformation, *Am. Assoc. Pet. Geol. Bull.*, *71*, 1414–1427.

Davis, E. E., H. Villinger, and T. Sun (2015), Slow and delayed deformation and uplift of the outermost subduction prism following ETS and seismogenic slip events beneath Nicoya Peninsula, Costa Rica, *Earth Planet. Sci. Lett.*, *410*, 117–127, doi:10.1029/98JB00162.

den Hartog, S. A. M., A. R. Niemeijer, and C. J. Spiers (2012), New constraints on megathrust slip stability under subduction zone P–T conditions, *Earth Planet. Sci. Lett.*, *353–354*, 240–252, doi:10.1016/j.epsl.2012.08.022.

den Hartog, S. A. M., and C. J. Spiers (2013), Influence of subduction zone conditions and gouge composition on frictional slip stability of megathrust faults, *Tectonophysics*, *600*, 75–90, doi:10.1016/j.tecto.2012.11.006.
Deng, X., and M. B. Underwood (2001), Abundance of smectite and the location of a plate-boundary fault, Barbados accretionary prism, *Geol. Soc. Am. Bull.*, *113*, 495–507, doi:10.1130/0016-7606.
Dixon, T. H., and J. C. Moore (2007), The seismogenic zone of subduction thrust faults: Introduction, in *The Seismogenic Zone of Subduction Thrust Faults*, edited by T. Dixon and J. C. Moore, pp. 2–14, Columbia Univ. Press, New York.
Ellis, S., Å. Fagereng, D. Barker, S. Henrys, D. Saffer, L. Wallace, C. Williams, and R. Harris (2015), Fluid budgets along the northern Hikurangi subduction margin, New Zealand: The effect of a subducting seamount on fluid pressure, *Geophys. J. Int.*, *202*, 277–297, doi:10.1093/gji/ggv127.
Expedition 316 Scientists (2009), Expedition 316 Site C0006, in *Proceedings of the Integrated Ocean Drilling Program*, vol. 314/315/316, pp. 1–124, Integrated Ocean Drilling Program Management International, Inc., Washington, D. C., doi:10.2204/iodp.proc.314315316.134.2009.
Fagereng, Å., G. W. B. Hillary, and J. F. A. Diener (2014), Brittle-viscous deformation, slow slip, and tremor, *Geophys. Res. Lett.*, *41*, 4159–4167, doi:10.1002/2014GL060433.
Gettemy, G. L., and H. J. Tobin (2003), Tectonic signatures in centimeter-scale velocity-porosity relationships of Costa Rica convergent margin sediments, *J. Geophys. Res.*, *108* (B10), 2494, doi:10.1029/2001JB000738.
Hyndman, R. D., M. Yamano, and D. A. Oleskevich (1997), The seismogenic zone of subduction thrust faults, *Isl. Arc*, *6*, 244–260, doi:10.1111/j.1440-1738.1997.tb00175.x.
Ikari, M. J., D. M. Saffer, and C. Marone (2007), Effect of hydration state on the frictional properties of montmorillonite-based fault gouge, *J. Geophys. Res.*, *112*, B06423, doi:10.1029/2006JB004748.
Ikari, M. J., B. M. Carpenter, C. Vogt, and A. J. Kopf (2016), Elevated time-dependent strengthening rates observed in San Andreas Fault drilling samples, *Earth Planet. Sci. Lett.*, *450*, 164–172, doi:10.1016/j.epsl.2016.06.036.
Ito, Y., and K. Obara (2006), Dynamic deformation of the accretionary prism excites very low frequency earthquakes, *Geophys. Res. Lett.*, *33*, L02311, doi:10.1029/2005GL025270.
Kameda, J., M. Shimizu, K. Ujiie, T. Hirose, M. Ikari, J. Mori, K. Oohashi, and G. Kimura (2015), Pelagic smectite as an important factor in tsunamigenic slip along the Japan Trench, *Geology*, *43*, 155–158, doi:10.1130/G35948.1.
Katayama, I., T. Kubo, H. Sakuma, and K. Kawai (2015), Can clay minerals account for the behavior of non-asperity on the subducting plate interface?, *Prog Earth Planet Sci*, *2*, 30, doi:10.1186/s40645-015-0063-4.
Kitajima, H., and D. M. Saffer (2012), Elevated pore pressure and anomalously low stress in regions of low frequency earthquakes along the Nankai Trough subduction megathrust, *Geophys. Res. Lett.*, *39*, L23301, doi:10.1029/2012GL053793.
Liu, Y., and J. R. Rice (2005), Aseismic slip transients emerge spontaneously in three-dimensional rate and state modeling of subduction earthquake sequences, *J. Geophys. Res.*, *110*, B08307, doi:10.1029/2004JB003424.
Logan, J. M., and K. A. Rauenzahn (1987), Frictional dependence of gouge mixtures of quartz and montmorillonite on velocity, composition and fabric, *Tectonophysics*, *144*, 87–108, doi:10.1016/0040-1951(87)90010-2.
Marone, C. (1998a), Laboratory-derived friction laws and their application to seismic faulting, *Annu. Rev. Earth Planet. Sci.*, *26*, 643–696.
Marone, C. (1998b), The effect of loading rate on static friction and the rate of fault healing during the earthquake cycle, *Nature*, *391*, 69–72, doi:10.1038/34157.
Marone, C., and C. H. Scholz (1988), The depth of seismic faulting and the upper transition from stable to unstable slip regimes, *Geophys. Res. Lett.*, *15*, 621–624, doi:10.1029/GL015i006p00621.
Marone, C., C. B. Raleigh, and C. H. Scholz (1990), Frictional behavior and constitutive modeling of simulated fault gouge, *J. Geophys. Res.*, *95*, 7007–7025, doi:10.1029/JB095iB05p07007.
Miyawaki, R., et al. (2010), Some reference data for the JCSS clay specimens [in Japanese with English abstract], *J. Clay Sci. Soc. Jpn.*, *48*, 158–198.
Moore, D. E., and D. A. Lockner (2007), Friction of the smectite clay montmorillonite: A review and interpretation of data, in *The Seismogenic Zone of Subduction Thrust Faults*, edited by T. Dixon and J. C. Moore, pp. 317–345, Columbia Univ. Press, New York.
Moore, D. E., D. A. Lockner, H. Tanaka, and K. Iwata (2004), The coefficient of friction of chrysotile gouge at seismogenic depths, *Int. Geol. Rev.*, *46*, 385–398, doi:10.2747/0020-6814.46.5.385.
Moore, J. C., and D. Saffer (2001), Updip limit of the seismogenic zone beneath the accretionary prism of southwest Japan: An effect of diagenetic to low-grade metamorphic processes and increasing effective stress, *Geology*, *29*, 183–186, doi:10.1130/0091-7613.
Morrow, C., B. Radney, and J. Byerlee (1992), Frictional strength and the effective pressure law of montmorillonite and illite clays, in *Fault Mechanics and Transport Properties of Rocks*, edited by B. Evans and T.-F. Wong, pp. 69–88, Academic Press, San Diego, Calif.
Park, J.-O., T. Tsuru, S. Kodaira, P. R. Cummins, and Y. Kaneda (2002), Splay fault branching along the Nankai subduction zone, *Science*, *297*, 1157–1160, doi:10.1126/science.1074111.
Pytte, A. M., and R. C. Reynolds (1988), The thermal transformation of smectite to illite, in *Thermal Histories of Sedimentary Basins*, edited by N. D. Naeser and T. H. McCulloh, pp. 133–140, Springer, New York.
Ranero, C. R., I. Grevemeyer, H. Sahling, U. Barckhausen, C. Hensen, K. Wallmann, W. Weinrebe, P. Vannucchi, R. von Huene, and K. McIntosh (2008), Hydrogeological system of erosional convergent margins and its influence on tectonics and interplate seismogenesis, *Geochem. Geophys. Geosyst.*, *9*, Q03S04, doi:10.1029/2007GC001679.
Saffer, D. M., and B. A. Bekins (2006), An evaluation of factors influencing pore pressure in accretionary complexes: Implications for taper angle and wedge mechanics, *J. Geophys. Res.*, *111*, B04101, doi:10.1029/2005JB003990.
Saffer, D. M., and C. Marone (2003), Comparison of smectite- and illite-rich gouge frictional properties: Application to the updip limit of the seismogenic zone along subduction megathrusts, *Earth Planet. Sci. Lett.*, *215*, 219–235, doi:10.1016/S0012-821X(03)00424-2.
Saffer, D. M., and H. J. Tobin (2011), Hydrogeology and mechanics of subduction zone forearcs: Fluid flow and pore pressure, *Annu. Rev. Earth Planet. Sci.*, *39*, 157–186, doi:10.1146/annurev-earth-040610-133408.
Saffer, D. M., and L. M. Wallace (2015), The frictional, hydrologic, metamorphic and thermal habitat of shallow slow earthquakes, *Nat. Geosci.*, *8*, 594–600, doi:10.1038/ngeo2490.
Saffer, D. M., M. B. Underwood, and A. W. McKiernan (2008), Evaluation of factors controlling smectite transformation and fluid production in subduction zones: Application to the Nankai Trough, *Island Arc*, *17*, 208–230, doi:10.1111/j.1440-1738.2008.00614.x.
Scholz, C. H. (1998), Earthquakes and friction laws, *Nature*, *391*, 37–42.
Scuderi, M. M., and C. Collettini (2016), The role of fluid pressure in induced vs. triggered seismicity: Insights from rock deformation experiments on carbonates, *Sci. Rep.*, *6*, 24852, doi:10.1038/srep24852.
Skarbek, R. M., A. W. Rempel, and D. A. Schmidt (2012), Geologic heterogeneity can produce aseismic slip transients, *Geophys. Res. Lett.*, *39*, L21306, doi:10.1029/2012GL053762.

Spinelli, G. A., D. M. Saffer, and M. B. Underwood (2006), Hydrogeologic responses to three-dimensional temperature variability, Costa Rica subduction margin, *J. Geophys. Res.*, *111*, B04403, doi:10.1029/2004JB003436.
Sposito, G., and R. Prost (1982), Structure of water adsorbed on smectites, *Chem. Rev.*, *82*, 553–573, doi:10.1021/cr00052a001.
Takahashi, M., K. Mizoguchi, K. Kitamura, and K. Masuda (2007), Effects of clay content on the frictional strength and fluid transport property of faults, *J. Geophys. Res.*, *112*, B08206, doi:10.1029/2006JB004678.
Tanikawa, W., H. Mukoyoshi, O. Tadai, T. Hirose, A. Tsutsumi, and W. Lin (2012), Velocity dependence of shear-induced permeability associated with frictional behavior in fault zones of the Nankai subduction zone, *J. Geophys. Res.*, *117*, B05405, doi:10.1029/2011JB008956.
Tembe, S., D. A. Lockner, and T.-F. Wong (2010), Effect of clay content and mineralogy on frictional sliding behavior of simulated gouges: Binary and ternary mixtures of quartz, illite, and montmorillonite, *J. Geophys. Res.*, *115*, B03416, doi:10.1029/2009JB006383.
Tesei, T., C. Collettini, B. M. Carpenter, C. Viti, and C. Marone (2012), Frictional strength and healing behavior of phyllosilicate-rich faults, *J. Geophys. Res.*, *117*, B09402, doi:10.1029/2012JB009204.
Tesei, T., C. Collettini, M. R. Barchi, B. M. Carpenter, and G. Di Stefano (2014), Heterogeneous strength and fault zone complexity of carbonate-bearing thrusts with possible implications for seismicity, *Earth Planet. Sci. Lett.*, *408*, 307–318, doi:10.1016/j.epsl.2014.10.021.
Tobin, H. J., and D. M. Saffer (2009), Elevated fluid pressure and extreme mechanical weakness of a plate boundary thrust, Nankai Trough subduction zone, *Geology*, *37*, 679–682, doi:10.1130/G25752A.1.
Underwood, M. B. (2007), Sediment inputs to subduction zones: Why lithostratigraphy and clay mineralogy matter, in *The Seismogenic Zone of Subduction Thrust Faults*, edited by T. H. Dixon and J. C. Moore, pp. 42–85, Columbia Univ. Press, New York.
Vrolijk, P. (1990), On the mechanical role of smectite in subduction zones, *Geology*, *18*, 703–707, doi:10.1130/0091-7613.
Wallace, L. M., and J. Beavan (2010), Diverse slow slip behavior at the Hikurangi subduction margin, New Zealand, *J. Geophys. Res.*, *115*, B12402, doi:10.1029/2010JB007717.
Wallace, L. M., S. C. Webb, Y. Ito, K. Mochizuki, R. Hino, S. Henrys, S. Y. Schwartz, and A. F. Sheehan (2016), Slow slip near the trench at the Hikurangi subduction zone, New Zealand, *Science*, *352*, 701–704, doi:10.1126/science.aaf2349.
Wang, K., and Y. Hu (2006), Accretionary prisms in subduction earthquake cycles: The theory of dynamic Coulomb wedge, *J. Geophys. Res.*, *111*, B06410, doi:10.1029/2005JB004094.